

Fault detection in engines through higher order spectral analysis of acoustic signatures

G. D. Meegan, H.R. Nelson, M. L. Barlett, and G. R. Wilson

*Applied Research Laboratories, The University of Texas at Austin,
P.O. Box 8029, Austin, Texas 78713-8029, USA*

meegan@arlut.utexas.edu barlett@arlut.utexas.edu wilson@arlut.utexas.edu

Abstract: This paper describes new engine fault detection methods that involve a higher order spectral analysis method known as the parametric spectral coherence (PSC). Measurements of radiated acoustic and vibrational signatures were conducted on a one-cylinder engine with a continuously worsening loss of cylinder compression. Compared to vibrational signatures, the radiated acoustic signatures provided the most dramatic indication of a loss of cylinder compression when PSC analysis was performed. It is demonstrated that the fault can be detected by simply monitoring the average spectral coherence or the peak spectral coherence of the acoustic signature, whereas the more traditional power spectral methods fail to detect the fault.

©1999 Acoustical Society of America

PACS numbers: 43.50.Yw, 43.60.Cg, 43.60.Lq

Introduction

The concept of machinery monitoring for the detection of faulty operation is not new. However, very little work has been done on monitoring and detecting faults in internal combustion engines. This deficiency seems to be due at least in part to the relative complexity of vibrational and acoustic signatures that are generated by internal combustion engines as compared with simpler rotating machinery. Nonetheless, if an effective method of early fault detection in engines can be developed, engine maintenance costs can be reduced and reliability increased through the use of a predictive maintenance (PdM) or condition based maintenance (CBM) method. With CBM, a repair is performed only as needed—for example, when the engine starts to run poorly. With PdM, maintenance is performed only when a need for repair is *predicted*, according to some method of detecting a problem with the engine. Thereby, maintenance costs decrease and reliability increases.¹

A typical application of machinery monitoring involves monitoring the vibration or acoustic power spectra of a machine for comparison with known spectra of normal and abnormal machinery. This method is widely used in detecting defects in rotating machinery such as turbines and electric motors. Some machinery monitoring devices are fully automated systems that continuously analyze power spectra. An alarm is triggered when an absolute spectral amplitude threshold is exceeded, indicating that a vibration at a specific frequency is unusually large.^{2,3} This concept is illustrated in Fig. 1 where a power spectral acceptance envelope, as defined from historical data, is used to define the normal operation of a machine. In this case, we see that the spectral lines at $3f_0$ and $5f_0$ have exceeded the acceptance threshold—this indicates that there may be a problem.

Unfortunately, power spectral analysis methods of detecting faults in internal combustion engines are much less reliable than detecting faults in turbines and electric motors. The vibrational and acoustic signatures of internal combustion engines typically contain a complicated series of harmonics of the engine firing rate, which, itself, varies with throttle level or engine RPM.⁴⁻⁶ In contrast, an electric motor typically operates at a fixed RPM and produces vibrations dominated by a single frequency equal to the rotation rate. The complicated spectral signatures of normally operating internal combustion engines make it

impossible to define a simple but effective spectral envelope for detecting faulty operation or imminent failure.

The application of higher order spectral analysis methods for the detection or classification of machinery faults has only recently been studied.^{7,8} Unlike a power spectral analysis, a higher order spectral analysis provides a quantitative measure of spectral coherences that may exist in a vibrational or acoustic signature. These spectral coherences are independent of spectral power and indicate the existence of a nonrandom phase relationship between frequency pairs. Here we shall apply a higher order spectral analysis technique known as the parametric spectral coherence C defined by⁷

$$C(\omega_1, \omega_2) = \frac{\langle A(\omega_1)A(\omega_2)e^{j[\phi(\omega_1) - \frac{\omega_1}{\omega_2}\phi(\omega_2)]} \rangle}{\sqrt{\langle A^2(\omega_1) \rangle \langle A^2(\omega_2) \rangle}} \tag{1}$$

where $\langle \rangle$ denotes time averaging, and $A(\omega)$ and $\phi(\omega)$ are the magnitude and phase of the Fourier transform of a time series $x(t)$ defined according to

$$x(t) = \int_{-\infty}^{\infty} A(\omega)e^{j\phi(\omega)} e^{j\omega t} d\omega \tag{2}$$

From Eq. (1), it is apparent that C is a function of frequency pairs ω_1 and ω_2 and ranges from zero to one. C is nonzero when the following parametric phase relationship exists:⁷

$$\phi(\omega_1) = \frac{\omega_1}{\omega_2}\phi(\omega_2) + \text{constant} \tag{3}$$

Therefore, unlike more common higher order spectral analyses (i.e., the bispectrum), the parametric spectral coherence does not require frequency pairs to be harmonically related. For example, an engine or motor with reduction gearing will produce nonharmonically related frequencies that would go undetected with the bispectrum, whereas the parametric spectral coherence will detect all coherent tonals.

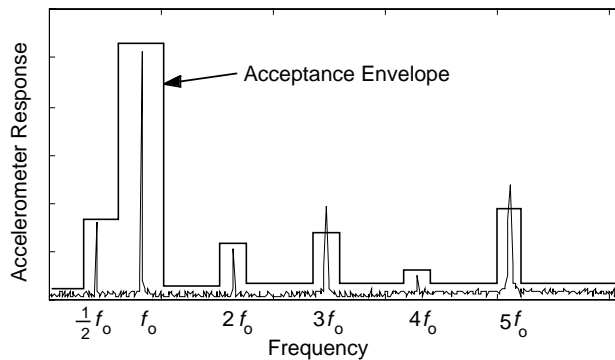


Fig. 1. Acceptance envelope method of power spectral fault detection.

Experiments

Figure 2 shows the experimental setup for the sound and vibration measurements on a single piston, two-stroke model airplane engine of 12.3 cm³ displacement, known as the Super Tigre 75. The propeller was removed for the measurements reported here. Probe tube microphones were used for insertion into the exhaust manifold and at the tailpipe. The on-axis farfield acoustic signature was measured with a 1/4 inch B&K microphone with a foam wind screen. Engine vibrations were also measured with an accelerometer that was attached to the engine mount. The axis of the accelerometer was placed in line with the axis of piston motion (perpendicular to the page in Fig. 2).

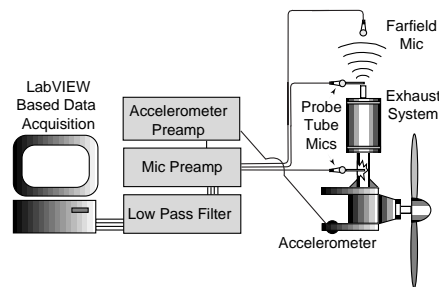


Fig. 2. Setup for measurements on the mono-cylinder engine.

An initial set of data on the mono-cylinder engine was collected under normal engine operation at constant throttle. Following these measurements, a fault was gradually induced in the engine by loosening the seal on the engine glow plug. This created a loss of compression in the cylinder by allowing some gas to escape from the glow plug tap on the cylinder head. On this particular engine, the glow plug could be loosened and tightened while collecting acoustic and vibrational data on the running engine. This allowed for measurement of progressive failure of the engine to the point that the engine stalls out.

Data analysis

In this section, data and analysis results are presented from the farfield acoustic measurements of a progressively worsening loss of cylinder compression in the one-cylinder engine. Results obtained from accelerometer and probe tube microphone sensors are qualitatively similar to those obtained from the farfield microphone. However, the farfield microphone sensor data yielded the most dramatic indication of faulty engine operation. This may be due to the particular type of fault we are studying here. Specifically, a loss of cylinder compression will have a direct effect on the pressure amplitude of the exhaust pulses generated with each combustion event. These exhaust pulses are the acoustic source that propagates through the exhaust system and to the farfield microphone. By comparison, one might expect that the engine block vibrations are only weakly coupled to the combustion events. Other types of faults, such as a main bearing failure, may be most strongly coupled to engine block vibrations and most easily detected through an analysis of vibrational signatures.

Power spectral plots of the farfield acoustic signature, averaged over consecutive time segments of the measurement, are shown in the left panel of Fig. 3. In general, the power spectrum is characterized by a complicated series of harmonics of the engine firing rate (120 Hz, in this case). Modeling results not reported here suggest that the underlying spectral noise floor is due largely to the acoustic response characteristics of the exhaust system. As the loss of compression worsens (towards the bottom of the figure), a suppression of distinct tonals is observed in the spectral data. Similar results were observed in the analysis of accelerometer and probe tube microphone data. Therefore, one may conclude that the fault is detectable through standard power spectral analysis methods. However, when an acceptance envelope is applied to the power spectral analysis results, fault detection is not successful. This failure is illustrated in the left panel of Fig. 3 where a possible acceptance envelope is overlaid on the power spectra—the faulty engine operation would go undetected by this method. Unlike much simpler rotating machinery, the series of harmonics that are present in normally functioning engines limit the usefulness of the power spectral acceptance envelope method. The effect of some faults in internal combustion engines is often a more subtle distortion of the power spectra that can be very difficult to detect by an automated vibration or noise monitoring system. For comparison, the results of a parametric spectral coherence analysis are shown in Fig. 4. The parametric spectral coherence is a function of frequency pairs ω_1 and ω_2 and is normalized to the power spectra according to Eq. (1). Notice that the diagonal (where $\omega_1 = \omega_2$) is identically 1, indicating that a tonal is always perfectly coherent

with itself. The loss of compression is found to be observable in the PSC analysis as a general loss of coherence. In the following section, methods for defining a simple coherence fault detector are presented that can be applied in much the same way as the acceptance envelope demonstrated in Fig. 1.

Coherence fault detector

The simplest type of coherence fault detector investigated here is a measure of the mean parametric spectral coherence. The mean parametric spectral coherence was calculated by simply averaging the coherence in Fig. 4, excluding the diagonal $\omega_1 = \omega_2$, over all frequency pairs to obtain a single measure of coherence in a given time interval. In this way, the analysis presented in Fig. 4 is reduced to the single point mean coherence measurements shown in Fig. 5. The mean coherence is well correlated to the progressive loss of cylinder compression as is detected by a loss of mean coherence. Therefore, mean coherence could be used as a simple metric for the development of automated methods of monitoring internal combustion engines for the detection of some types of faults. Two approaches are suggested: (1) A mean coherence threshold could be defined as shown in Fig. 5, based on machine history. A fault alarm would then be triggered when the mean coherence falls below the acceptable limit. (2) Trending methods could also be applied that may not require knowledge of machine history. For example, the rate of change in the mean coherence (the slope in Fig. 5) could be monitored so that a sudden change would indicate an engine fault.

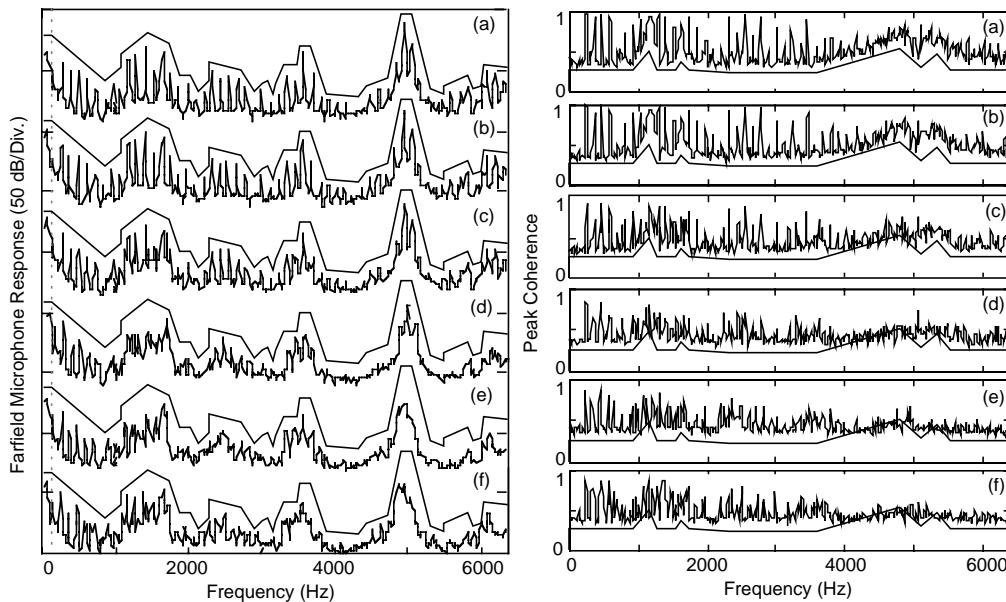


Fig. 3. Analysis of farfield acoustic signatures at time intervals (a) 0 to 4.8 seconds, (b) 4.8 to 9.6 seconds, (c) 9.6 to 14.4 seconds, (d) 14.4 to 19.2 seconds, (e) 19.2 to 24.0 seconds, and (f) 24.0 to 28.8 seconds. The loss of cylinder compression begins at 8 seconds and gradually increases. Left: Consecutive plots of the power spectral average as calculated from the farfield microphone measurement on the one-cylinder engine. The microphone was placed 57 cm from the tailpipe. A suppression of spectral lines is observed above 1 kHz when there is a loss of cylinder compression. The engine firing rate is 120 Hz and is indicated by the vertical dashed line. The power spectral acceptance envelope method fails to detect the fault. Right: The parametric spectral coherence was collapsed to a simpler plot of peak spectral coherence as a function of a single frequency. A $\Delta\omega = 200$ Hz main lobe mask was applied. The peak spectral coherence acceptance envelope method was successful in detecting the presence of a fault.

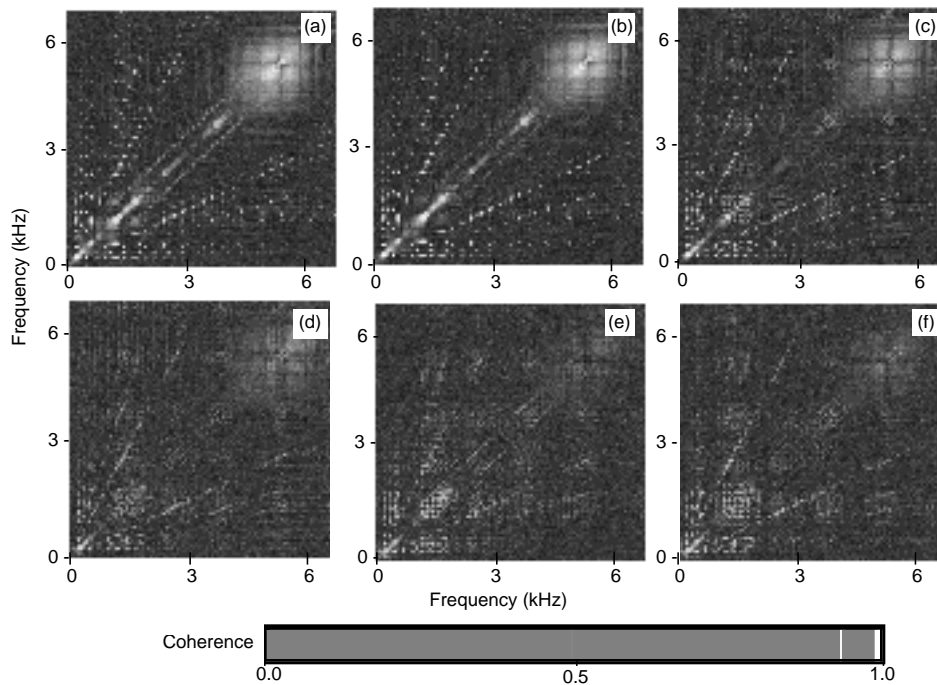


Fig. 4. The parametric spectral coherence was calculated for the farfield microphone measurements on the mono-cylinder engine at consecutive time intervals. A substantial loss of coherence occurs after the one-cylinder engine loss of compression at 8 seconds. The consecutive time intervals are: (a) 0 to 4.8 seconds, (b) 4.8 to 9.6 seconds, (c) 9.6 to 14.4 seconds, (d) 14.4 to 19.2 seconds, (e) 19.2 to 24.0 seconds, and (f) 24.0 to 28.8 seconds.

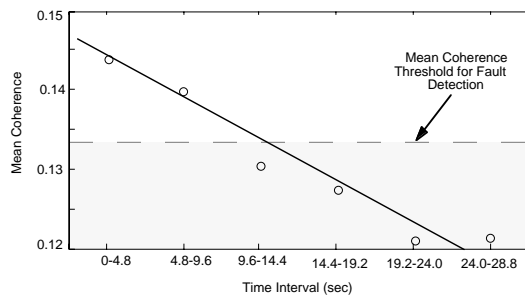


Fig. 5. The mean parametric spectral coherence was applied as a method of detecting the loss of compression. The dashed line specifies a coherence threshold alarm that is capable of detecting the fault.

The parametric spectral coherence can be plotted as a function of a single frequency to generate a waterfall plot, as is commonly used to track changes in the power spectra. The peak coherence C_p is defined here as a function of ω_l according to

$$C_p(\omega_l) = C(\omega_l, \omega_2 = \omega_{max}), \quad \omega_l \neq \omega_{max} \tag{4}$$

where ω_{max} is the value of ω_2 that has the *maximum* coherence at coordinate $\omega_l \neq \omega_2$. Collapsing Fig. 4 according to Eq. (4) results in the loss of distinct spectral peaks that are obvious in Fig. 4. This difficulty is because the peak coherence is dominated by the response

of the parametric spectral coherence near $\omega_1 = \omega_2$ (near the diagonal in Fig. 4). Although Eq. (4) requires $\omega_1 \neq \omega_2$, the $\omega_1 = \omega_2$ self-coherent tonals result in strong sidelobes in the two-dimensional space (ω_1, ω_2) . Therefore, the sidelobes near $\omega_1 = \omega_2$ should be masked before calculating a peak coherence at a frequency ω_1 . This calculation was accomplished by excluding the coherence for $|\omega_1 - \omega_2| < \Delta\omega$ so that we calculate the peak coherence as a function ω_1 according to

$$C_p(\omega_1) = C(\omega_1, \omega_2 = \omega_{max}), \quad |\omega_1 - \omega_{max}| > \Delta\omega \quad (5)$$

where $\Delta\omega$ is the width of the $\omega_1 = \omega_2$ sidelobe to be nulled.

In the right panel of Fig. 3, we present the peak coherence as calculated from Eq. (5) with a sidelobe nulling of $\Delta\omega = 200$ Hz. We find that the resulting plots of peak coherence show clear tonal peaks corresponding to harmonics of the engine firing rate. As the loss of compression increases, we see clear evidence in the peak coherence analysis. In the right panel of Fig. 3, we also demonstrate how a lower limit acceptance envelope (minimum coherence criteria as a function of ω) successfully detects the fault when coherences drop below normal levels. Unlike the standard power spectral acceptance envelope method demonstrated on the left panel of Fig. 3, the peak coherence envelope provides effective fault detection.

Summary and conclusions

A series of acoustic measurements was conducted on properly functioning internal combustion engines and engines with progressively worsening faults. Results indicate that it is possible to detect faulty engine operation by monitoring either the power spectra or the parametric spectral coherence. However, standard approaches such as a power spectral acceptance envelope method fail to detect the fault. By comparison, PSC analysis was shown to provide new methods of fault detection that could easily be automated. The mean spectral coherence and peak spectral coherence analysis methods presented here could provide the basis for automated fault detection and classification systems for a wide range of machinery types.

Acknowledgments

This work was supported by the Office of Naval Research, contract number N00014-96-1-0298-7.

References

- ¹ E. F. Pardue, K. R. Plety, and R. Moore, "Elements of reliability-based machinery maintenance," *Sound and Vib.*, 14-20, May (1992).
- ² R. M. Jones, "A guide to the interpretation of machinery vibration measurements—Part I," *Sound and Vib.*, 24-35, May (1994).
- ³ R. M. Jones, "A guide to the interpretation of machinery vibration measurements—Part II," *Sound and Vib.*, 12-20, September (1994).
- ⁴ M. L. Munjal, *Acoustics of Ducts and Mufflers with Application to Exhaust and Ventilation System Design*, (Wiley, New York, 1987).
- ⁵ R. Hickling and M. M. Kamal, *Engine Noise: Excitation, Vibration, and Radiation*, (Plenum, New York, 1982).
- ⁶ D. E. Baxa, *Noise Control in Internal Combustion Engines*, (Wiley, New York, 1982).
- ⁷ K. W. Baugh, "Parametric phase coupling in the vibration spectra of rolling element bearings," *Mech. Systems and Signal Proc.*, 215-228, 8, No. 2 (1994).
- ⁸ G. D. Meegan, H. R. Nelson, M. L. Barlett, and G. R. Wilson, "Analysis of engine noise for application in predictive maintenance," *J. Acoust. Soc. Am.*, **101**, No. 5, Pt. 2, 3029, (1997).